Mutual Correction of Faulty PCNA Subunits in Temperature-Sensitive Lethal *mus209* Mutants of *Drosophila melanogaster*

Daryl S. Henderson,* Ulrich K. Wiegand,† David G. Norman‡ and David M. Glover*

**CRC Cell Cycle Genetics Group, Department of Genetics, University of Cambridge, Cambridge CB2 3EH, United Kingdom, †Department of Anatomy and Physiology, and ‡Department of Chemistry, University of Dundee, Dundee DD1 5EH, United Kingdom*

Manuscript received September 3, 1999
Accepted for publication December 28, 1999

ABSTRACT

Proliferating cell nuclear antigen (PCNA) functions in DNA replication as a processivity factor for polymerases δ and ε, and in multiple DNA repair processes. We describe two temperature-sensitive lethal alleles (*mus209*^{B1} and *mus209*^{2735}) of the Drosophila PCNA gene that, at temperatures permissive for growth, result in hypersensitivity to DNA-damaging agents, suppression of position-effect variegation, and female sterility in which ovaries are underdeveloped and do not produce eggs. We show by mosaic analysis that the sterility of *mus209*^{B1} is partly due to a failure of germ-line cells to proliferate. Strikingly, *mus209*^{B1} and *mus209*^{2735} interact to restore partial fertility to heteroallelic females, revealing additional roles for PCNA in ovarian development, meiotic recombination, and embryogenesis. We further show that, although *mus209*^{B1} and *mus209*^{2735} homozygotes are each defective in repair of transposase-induced DNA double-strand breaks in somatic cells, this defect is substantially reversed in the heteroallelic mutant genotype. These novel mutations map to adjacent sites on the three-dimensional structure of PCNA, which was unexpected in the context of this observed interallelic complementation. These mutations, as well as four others we describe, reveal new relationships between the structure and function of PCNA.

PROLIFERATING cell nuclear antigen (PCNA) functions in DNA replication as a processivity factor for two DNA polymerases, δ (pol δ) and ε (pol ε; reviewed by Kelman 1997; Tsurimoto 1998). It also participates in multiple repair processes: nucleotide excision repair (Nichols and Sancar 1992; Shivji *et al.* 1992), base excision repair (Matsumoto *et al.* 1994; Frosina *et al.* 1996; Klungland and Lindahl 1997), mismatch repair (Johnson *et al.* 1996; Umar *et al.* 1996; Gu *et al.* 1998), postreplication repair (Torres-Ramos *et al.* 1996), and double-strand break (DSB) repair (Henderson and Glover 1998; Holmes and Haber 1999).

The three-dimensional structures of both *Saccharomyces cerevisiae* PCNA and human PCNA are virtually superimposable even though the molecules share just 35% amino acid identity (Krishna *et al.* 1994; Gulbis *et al.* 1996). Three PCNA molecules, each consisting of two topologically similar domains, interact head to tail to form a ring-shaped structure suitable for encircling and tracking along duplex DNA. The efficient loading of trimers of PCNA onto DNA requires the five-subunit protein replication factor C (RF-C) and ATP as a source of energy. The large (~140 kD) subunit of human RF-C contains a DNA-binding domain and two distinct PCNA-binding domains, one at the N terminus and the other located centrally. The latter domain may be conserved in the four small (36, 37, 38, and 40 kD) RF-C subunits (Fotedar *et al.* 1996; Mossi *et al.* 1997). These biochemical findings are supported by genetic evidence of an interaction between PCNA and RF-C in *S. cerevisiae*: five independent mutations isolated as suppressors of cold-sensitive alleles of *CDC44*, which encodes the large subunit of RF-C, were found to reside in the PCNA gene *POL30* (McAlear *et al.* 1994).

The two domains of each PCNA monomer are linked by an interdomain connector loop (Figure 1). Each domain contains two α helices, so that a total of 12 helices line the inside of the trimeric ring girdled by a β sheet that extends across both interdomain and intermolecular boundaries. Warbrick and colleagues (1995) showed that the connector region of PCNA is necessary for the binding of the CDK inhibitor p21, and the crystal structure of human PCNA complexed to a C-terminal segment of p21 confirmed that the two polypeptides interact to form a β sheet in this region (Gulbis *et al.* 1996). FEN-1, DNA ligase I, DNA-(cytosine-5)methyltransferase and XPG endonuclease each compete with p21 for binding to the interdomain connector (Chuang *et al.* 1997; Gary *et al.* 1997; Warbrick *et al.* 1997; Montecucco *et al.* 1998), and pol δ also binds to a segment of this loop (Roos *et al.* 1996; Oku *et al.* 1998; Zhang *et al.* 1998).

Mutagenesis of *S. cerevisiae* and *Schizosaccharomyces pombe* PCNAs has identified a number of single, double, and quadruple alanine substitution mutants with moderate growth defects and/or enhanced sensitivity to DNA-damaging agents (Ayyagari *et al.* 1995; Arroyo

Corresponding author: Daryl S. Henderson, University of Cambridge, Department of Genetics, Downing St., Cambridge CB2 3EH, United Kingdom. E-mail: dsh25@mole.bio.cam.ac.uk

et al. 1996; Arroyo and Wang 1998). Substitution by alanine of any one of nine highly conserved, basic, α-helical residues at the inner surface of the ring of human PCNA impaired pol δ stimulation, but had no effect on the activation of RF-C ATPase. This selective defect was ascribed to problems of PCNA clamping onto DNA (Fukuda *et al.* 1995). In contrast, mutation of acidic, highly conserved surface residues to alanine was largely without effect. Significantly, deletion of the last eight residues of human PCNA abolished RF-C ATPase stimulation but had no effect on pol δ activation, implicating the very C terminus of PCNA in RF-C binding (Fukuda *et al.* 1995; see also Mossi *et al.* 1997). The formation of trimers is abolished by mutation of a conserved residue, tyrosine 114 (Y114A), located in domain 1 at the intermolecular interface (Jónnson *et al.* 1995). This particular mutant form of PCNA also failed to activate DNA synthesis, suggesting that only trimeric PCNA can productively interact with pol δ. Random mutagenesis also generated a similar trimerization-defective cold-sensitive mutant in *S. cerevisiae* (S115P) that is highly sensitive to DNA-damaging agents at temperatures permissive for growth. Fourteen additional budding yeast mutants isolated by random mutagenesis have been categorized into one of two phenotypic classes: those sensitive to the DNA-damaging agent methyl methanesulfonate (MMS) and those both MMS sensitive and cold sensitive for growth (Amin and Holm 1996). The mutated residues in the cold-sensitive mutants were found to be clustered near the interdomain region of the monomer, whereas those of the strictly MMS-sensitive mutants were found to be dispersed. Apparently, MMS-induced lesions in DNA are repaired by activities that are especially intolerant of even minor alterations to PCNA structure.

PCNA in *Drosophila melanogaster* is encoded by the gene *mus209* (Henderson *et al.* 1994). Most extant mutations in *mus209* result in nonconditional lethality. However, a multitude of other phenotypic effects are associated with reduced PCNA activity in two temperature-sensitive (ts) lethal *mus209* mutants. $mus209^{B1}$ homozygous females, for example, are sterile at temperatures permissive for growth. Mutant embryos and larvae are hypersensitive to DNA-damaging agents, such as ionizing radiation and MMS, reflecting PCNA's central role in DNA repair. These mutants also fail to repair double-strand breaks in DNA that result from mobilization of transposable *P* elements (Henderson and Glover 1998). Furthermore, $mus209^{B1}$ is a recessive suppressor of the gene-silencing phenomenon known as position-effect variegation (PEV), which suggests a role for PCNA in the assembly and/or maintenance of chromatin structure (Henderson *et al.* 1994). This hypothesis has recently been lent further support by the observations of genetic interactions between *mus209* and members of the *Polycomb*-group class of homeotic genes, including *cramped* and *Polycomb* itself (Yamamoto *et al.* 1997; Y. Yamamoto, personal communication), which regulate gene expression through higher-order chromatin structures (reviewed by Pirrotta 1997). In this work, we report the molecular defects in six ethyl methanesulfonate (EMS)-induced *mus209* mutants, including the first heat-sensitive lethal alleles of PCNA to be described in any organism, which are of particular interest since they show interallelic complementation. The placement of these novel heat-sensitive mutations onto the three-dimensional structure of PCNA identifies a new functional domain within the PCNA trimer.

MATERIALS AND METHODS

Drosophila stocks and culture conditions: The origins of the *mus209* alleles are described in Henderson *et al.* (1994). For full descriptions of the visible mutations and balancer chromosomes used in this study, refer to FlyBase (1999). The following two strains require special mention. The balancer stock *TSTL14* was derived from a reciprocal translocation involving chromosomes 2 and 3 (see Gatti and Goldberg 1991). *TSTL14* carries the dominant larval marker *Tb. Fs(2)D* is a germ-line-dependent dominant female sterile mutation (Yarger and King 1971) located distally on the right arm of chromosome 2 (Schüpbach 1982). It is maintained as a balanced stock consisting of *T(1;2)Bld/Fs(2)D* males and *T(1;2)OR64, y* females. *Fs(2)D* was kindly provided by T. Schüpbach. All experiments were carried out at 22 ± 1°, which is the permissive temperature for growth of $mus209^{B1}$ and $mus209^{2735}$ (Henderson *et al.* 1994).

DNA sequencing: Genomic DNA for sequencing was obtained from homozygous adults ($mus209^{B1}$ and $mus209^{D\text{-}1368}$) or hemizygous larvae ($mus209^{36}$, $mus209^{157}$, $mus209^{775}$, and $mus209^{2735}$) using standard procedures. Hemizygous larvae were generated by crossing $mus209^{x}/TSTL14$ females with *Df(2R)173/TSTL14* males and selecting non-Tb offspring. Templates for sequencing were obtained by PCR amplification of the entire *mus209* coding region and were either sequenced directly using a dsDNA cycle sequencing system (GIBCO BRL, Gaithersburg, MD) ($mus209^{B1}$ and $mus209^{D\text{-}1368}$) or cloned into pGEM-T vector (Promega, Madison, WI) and sequenced by conventional methods (United States Biochemicals, Cleveland; all six mutants). Initially, both strands of each allele were sequenced in their entirety. Mutations were verified by sequencing no fewer than three independently amplified and cloned templates using primers flanking the mutated base. In addition to the unique missense mutations reported here, all six mutants share a number of differences from a previously published sequence of the Drosophila PCNA gene (Yamaguchi *et al.* 1990): 52G → A (5′ untranslated region); 216A → T and 253T → C (intron); 317C → T, 329T → C, and 542A → G (silent substitutions in coding region). Presumably, these are strain-specific polymorphisms.

Computer modeling: Initial models of PCNA from *Drosophila melanogaster* were generated using the program MODELLER 4 (Sali and Blundell 1993). Alignment of the sequences from the structures, with Brookhaven Protein Databank id 1AXC and 1PLQ, with the sequence for Drosophila PCNA was used as the starting point for the generation of a homology bases model using standard techniques. Mutation positions were visualized and structures were manipulated within the graphics package InsightII (MSI). Construction of back-to-back models of PCNA was achieved by interactive computer graphical docking followed by energy minimization using the software X-PLOR (Axel T. Brünger, Yale University).

Ovary analysis: β-*Galactosidase staining:* Ovaries homozygous for both the X-linked *ovo-lacZ* reporter 46.2 (Mével-Ninio *et al.* 1995) and either *mus209*^{B1} or *mus209*^{2735} were prepared following Mével-Ninio *et al.* (1995) with minor modifications. Briefly, ovaries were dissected in phosphate-buffered saline (PBS)/0.1% Triton X-100, rinsed in PBS, and fixed in PBS/2.5% glutaraldehyde for 20 min at room temperature with gentle agitation. They were washed in two changes of PBS/0.3% Triton X-100, 30 min each, with gentle agitation, and then incubated overnight at 37° in staining solution (PBS, 0.3% Triton X-100, 1 mm $MgCl_2$, 0.5 mm $K_3Fe(CN)_6$, 0.5 mm $K_4Fe(CN)_6$, 0.2% X-gal). Ovaries were placed in chamber slides and photographed through a stereomicroscope.

Hoechst staining: Ovaries were fixed and then stained with the DNA fluorochrome Hoechst 33342 (Sigma, St. Louis) following the procedure of Bellen and Kiger (1988), except that PBS was used in place of buffer A.

Induction of germ-line clones by mitotic recombination: Germ line clones homozygous for *mus209*^{B1} were induced in *mus209*^{B1}/*Fs(2)D* females by the dominant female-sterile technique (Wieschaus 1980) according to the procedure of Schüpbach (1982). To obtain females for X-irradiation, *T(1;2)Bld*/*Fs(2)D* males were crossed to *cn bw* females. Their *Fs(2)D*/*cn bw* male progeny were mated to *b pr cn mus209*^{B1} *bw*/*CyO* or *b pr cn bw*/*CyO* females, and 48 ± 4-hr-old larvae from each cross were irradiated with X rays (8.5 Gy) under conditions described previously (Banga *et al.* 1986). Virgin *b pr cn mus209*^{B1} *bw*/*Fs(2)D* or *b pr cn bw*/*Fs(2)D* females were placed 10 to a vial with 5 *cn bw* males. Females of either genotype are sterile unless *Fs(2)D* has been eliminated from a germ cell by an induced mitotic recombination event. In *mus209*^{B1}/*Fs(2)D* females, crossing over proximal to *mus209*^{B1} and *Fs(2)D* will render a gonial cell precursor homozygous for both *mus209*^{B1} and *Fs(2)D*$^{+}$ (Figure 2A, crossovers 1 and 2). Since the *mus209* locus occupies a distal position on 2R (at 56F5-15; Henderson *et al.* 1994), we expected that the vast majority of induced crossovers would generate germ lines of that genotype. In practice, however, such mosaic females can be identified unambiguously only where the crossover has occurred proximal to *cn* (Figure 2A, crossover 1); germ lines of that class (if fertile) produce only white-eyed (cn bw) progeny when mated to *cn bw* males. A control female was required to produce at least 12 progeny, all having white eyes, before it was concluded that the crossover had occurred proximal to *cn* (Schüpbach 1982). (We estimate that no fewer than 11 of the 23 "fertile" *mus209*^{B1}/*Fs(2)D* females would have carried a germ line homozygous for *mus209*^{B1}. This conservative estimate derives from the observation that crossovers occurred proximal to *cn* in ~50% (8/15) of control females that produced ≥12 progeny.) Cultures were examined daily for evidence of fertility (larval activity) for a period of ≥10 days. Individual females from fertile cultures were transferred to separate vials and their progeny were counted and classified after eclosion. Note: Fertility was restored to six *mus209*^{B1}/*Fs(2)D* females as a result of reversion of *Fs(2)D* and not by mitotic recombination. This conclusion is based on recovery of phenotypically wild-type and cn offspring whose presence cannot be explained by somatic crossing over without invoking the occurrence of extremely rare multiple recombination events. Others have observed revertants of *Fs(2)D*, although at a lower frequency than that found here (T. Schüpbach, personal communication). The *Fs(2)D* revertant females generated in this study were not analyzed further.

Fixation and immunostaining of embryos: Embryos from 2-hr collections were dechorionated in 2.5% sodium hypochlorite solution for 3 min, rinsed in PBS/0.1% Triton X-100 (PBST), then in PBS or distilled water, and fixed in 37% formaldehyde/heptane for 0.5–1 hr with gentle agitation. After fixation, embryos were transferred to microscope slides to which double-sided adhesive tape had been attached, and their vitellin membranes were removed by hand under PBS. Embryos were incubated in blocking solution [PBST/10% fetal calf serum (FCS)] for 1 hr. Blocking solution was replaced with fresh PBST/FCS containing primary antibodies [rat α-tubulin, YL1/2 monoclonal antibodies (Jackson Immunoresearch, West Grove, PA), 1:10 dilution; rabbit α-Drosophila PCNA polyclonal antiserum (see below), 1:250–1:500 dilution] and 100 μg/ml RNase A, and embryos were incubated overnight at 4°. Embryos were washed for 2 hr (30-min changes) in PBST and then incubated in PBST/FCS containing secondary antibodies [donkey α-rat Cy5-conjugated IgG (Jackson Immunoresearch), 1:100 dilution; goat α-rabbit fluorescein-conjugated IgG (Jackson Immunoresearch), 1:500 dilution] for 2 hr at room temperature or overnight at 4°. Embryos were washed as described above, rinsed in PBS, stained with the DNA fluorochrome propidium iodide, and mounted in Mowiol mounting medium. Images were recorded using an MRC 1024 laser scanning confocal microscope (Bio-Rad, Richmond, CA).

Production of polyclonal antiserum against *D. melanogaster* PCNA: For expression of a recombinant antigen, the plasmid pQE30/H-PCNA encoding $(His)_6$-tagged *D. melanogaster* PCNA was generated. An appropriate cDNA fragment was amplified by PCR using the primers 5′-cacggatccgactacaaggacgacgatga caagatgttcgaggcacgcctgggtc-3′ and 5′-cgacgtaagcttatgtctcgttgt cctcgatcttg-3′ (restriction sites *Bam*HI and *Hin*dIII are underlined, respectively) and a full-length *mus209* cDNA as template (Henderson *et al.* 1994). The restriction enzyme sites introduced into the primers were utilized for cloning the amplified product into the expression vector pQE30 (Qiagen, Chatsworth, CA). The sequence of the cloned insert was verified by sequencing both strands. *Escherichia coli* strain M15[pREP4] was transformed with pQE30/H-PCNA and used to inoculate 2 liters of LB medium. Cells were grown at 30° to A_{600} of 0.5. Recombinant protein expression was induced by adding 0.5 mm isopropyl thiogalactoside and growing the culture at room temperature for 1.5 hr. Cells were harvested by centrifugation and the pellet was redissolved in 25 ml lysis buffer (50 mm NaH_2PO_4, 10 mm Tris-HCl, 100 mm NaCl, pH 8.0). Lysis was carried out by freeze thawing the cells and subsequent sonication on ice. Debris and insoluble material were pelleted by centrifugation at 12,000 *g*. The clear crude extract was loaded onto a TALON metal affinity resin column (Clontech, Palo Alto, CA) equilibrated with 10 volumes of lysis buffer. The column was washed with 30 ml lysis buffer and 30 ml wash buffer (50 mm NaH_2PO_4, 100 mm NaCl, pH 7.0). The recombinant protein was eluted with 10 ml of elution buffer (50 mm NaH_2PO_4, 20 mm PIPES, 100 mm NaCl, pH 5.9). Aliquots (0.5 ml) were collected and analyzed by SDS-PAGE (Ausubel *et al.* 1998). The fractions containing the purified recombinant $(His)_6$-PCNA were pooled and protein concentration was determined by Bradford assay (Bio-Rad). Purified $(His)_6$-PCNA (150 mg) was dissolved in 1 ml MPL+TDM+CWS adjuvant (Sigma) and injected into a rabbit. This was repeated three more times at 28-day intervals. Serum was prepared from whole blood (Harlow and Lane 1988) and analyzed by Western blotting (Ausubel *et al.* 1998).

Analysis of meiotic recombination: Meiotic recombination was measured in *mus209*^{B1}/*mus209*^{2735} females using a multiply mutant chromosome 2 marked with the recessive visible mutations *al* (0.4), *dp* (13.0), *b* (48.5), *pr* (54.5), and *cn* (57.5). The numbers in parentheses refer to the genetic map position of each locus, as listed in Lindsley and Zimm (1992). To generate females for analysis, *al dp b pr cn mus209*^{2735}/*CyO* males were mated to *mus209*^{B1}/*CyO* females. F_1 *al dp b pr cn mus209*^{2735}/+ + + + + *mus209*^{B1} females were collected from that cross

and mated to *al dp b pr cn* homozygous males. F_2 progeny were counted and classified according to phenotype.

Analysis of double-strand break repair: Analysis of repair of *P*-element transposase-induced DNA double-strand breaks was carried out as described in Henderson and Glover (1998) and Henderson (1999) following Banga *et al.* (1991).

RESULTS

Mapping the mutated residues in two heat-sensitive lethal PCNA mutants in three dimensions: All the numerous temperature-sensitive (ts) mutants of PCNA recovered in the yeasts are cold sensitive for growth. The finding of two heat-sensitive EMS-induced mutants of Drosophila, *mus209*^{B1} and *mus209*^{2735}, thereby offered the opportunity to look at potentially novel aspects of the relationship between structure and function of the PCNA molecule. In addition, the mutants provide a means for studying the requirement for the protein during the development of a multicellular eukaryote. Animals homozygous for either of these ts alleles are viable at 22°, but fail to complete development when grown at 29°, dying as pupae. Animals heterozygous for a chromosome carrying either of these ts alleles and either a deletion or lethal EMS mutation of *mus209* die during development at 22°, usually as pupae (Henderson *et al.* 1994). This is in contrast to hemizygotes of nonconditional lethal mutants, which die usually as embryos or first instar larvae (see below). However, the most conspicuous phenotype in ts mutants raised under conditions permissive for growth is female sterility. Females homozygous for either *mus209*^{B1} or *mus209*^{2735} do not produce eggs. Strikingly, heteroallelic *mus209*^{B1}/*mus209*^{2735} females are partially fertile, yielding a small number of progeny able to develop to adulthood (Henderson *et al.* 1994). We sought to determine the molecular lesions in these PCNA molecules, and to explore their mutant phenotype in further depth to examine the extent of this interallelic complementation.

We determined the mutated residues in these two *mus209* mutants by DNA sequencing and then positioned the substitutions on the three-dimensional structure of Drosophila PCNA modeled on the crystal structure of yeast PCNA (Krishna *et al.* 1994). The ts mutant *mus209*^{B1} carries a proline-to-leucine substitution at position 140 (P140L). P140 is a highly conserved residue located at a bend in the PCNA main chain that marks the boundary between β strand A_2 (βA_2) and α helix A_2 (αA_2; Figure 1). The introduction of leucine at position 140 might perturb one or both of these structural elements, the deformations possibly being more severe at higher (*i.e.*, restrictive) temperatures. Another possi-

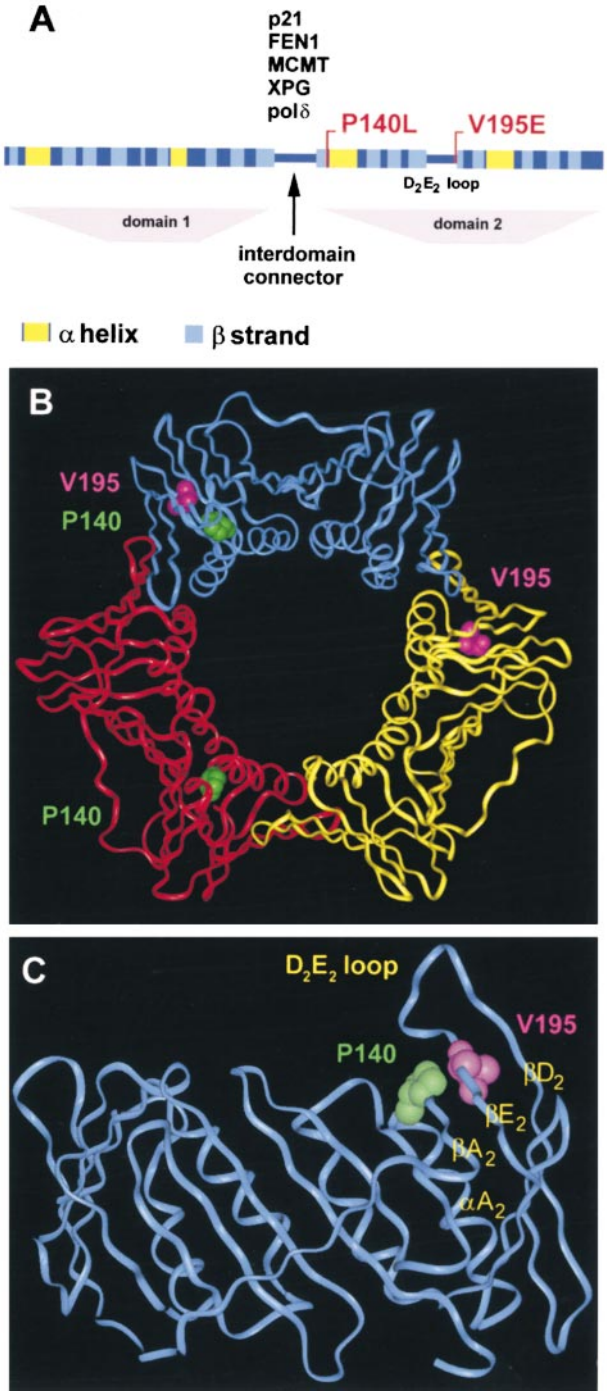

Figure 1.—Diagrammatic representations of PCNA. (A) Cartoon of a PCNA monomer showing its two domains, secondary structural elements (α helix, yellow; β strand, light blue), and known major sites of interaction of PCNA-binding molecules. (Some other points of contact are not indicated; *e.g.*, see Jónsson *et al.* 1998.) P140L and V195E denote the amino acid changes in *mus209*^{B1} and *mus209*^{2735}, respectively. (B) Computer-generated 3-D ribbon model of a PCNA trimer showing the positions of P140 (green) and V195 (crimson) on individual monomers colored red and yellow, respectively. The third monomer (blue) is a hypothetical molecule showing the relative positions of the two mutated residues. (C) Side-view of a PCNA monomer showing residues P140 and V195. Note their proximity to one another and to the D_2E_2 loop protruding from one face. αA_2 denotes the A_2 α helix; βA_2, βD_2, and βE_2 denote β strands.

ble effect of P140L is suggested by our analysis of the second heat-sensitive mutant, *mus209*^{2735}, whose phenotype we show below is identical to that of *mus209*^{B1}. Although the valine-to-glutamate substitution at position 195 (V195E) carried by *mus209*^{2735} is some 55 amino acids C terminal to P140, on the three-dimensional structure, P140 in βA_2 is packed against V195 at the N terminus of the adjacent antiparallel strand βE_2 (Figure 1). This raises the possibility that both mutants cause a similarly localized structural perturbation, possibly involving the D_2E_2 loop. This protruding loop has been likened to a molecular "handle" that is postulated to be a likely site of interaction between PCNA and other proteins (Krishna *et al.* 1994).

Cell proliferation defects in the germ line cause agametic sterility of *mus209* females: We wished to determine the developmental defect resulting in a failure of *mus209*^{B1} and *mus209*^{2735} homozygous females to produce eggs. In contrast to the wild type, gross anatomical examination of the ovaries from *mus209*^{B1} and *mus209*^{2735} homozygous adults revealed them to be small and poorly developed. They appeared to be partitioned into ovarioles, but these were rudimentary and obviously devoid of late-stage egg chambers. We wondered whether these ovaries could be missing germ cells and searched for the presence of these by incorporating into both mutant lines an ovo-β-galactosidase reporter specifically expressed in germ-line cells. This revealed the presence of only stem cells and early stage egg chambers, reminiscent of ovaries from pupae (King 1970), as though egg chambers had undergone developmental arrest (not shown).

The ability of germ-line cells to proliferate can also be tested by using X-ray-induced recombination to generate a homozygous *mus209*^{B1} mutant germ line within an otherwise functionally wild-type ovarian soma. To achieve this, we employed a chromosome carrying the dominant female sterile mutation *Fs(2)D* (Wieschaus 1980) to block oogenesis in germ-line cells not undergoing mitotic recombination (Figure 2). Cultures containing *mus209*^{B1}/*Fs(2)D* or *mus209*$^{+}$/*Fs(2)D* female larvae were irradiated with X rays to induce recombination in the developing germ line. Crossing over proximal to *mus209*^{B1} and *Fs(2)D* (Figure 2A, regions 1 and 2) will yield germ-line cells of the desired genotype, *i.e.*, homozygous for both *mus209*^{B1} and *Fs(2)D*$^{+}$. The results of this clonal analysis demonstrate that the defective PCNA in *mus209*^{B1} very poorly sustains development of the female germ line. The frequency of induced fertility was sixfold lower for *mus209*^{B1} females (0.9%) compared to *mus209*$^{+}$ controls (5.7%; Table 1). More importantly, fecundity differed dramatically between those two genotypes: *mus209*^{B1}/*Fs(2)D* mosaic females produced on average only 1.5 ± 0.8 viable progeny, whereas control females produced on average 14.4 ± 14.3 progeny (Figure 2, B and C). Indeed, whereas more than half (15/29) of the control females produced 12 or more progeny

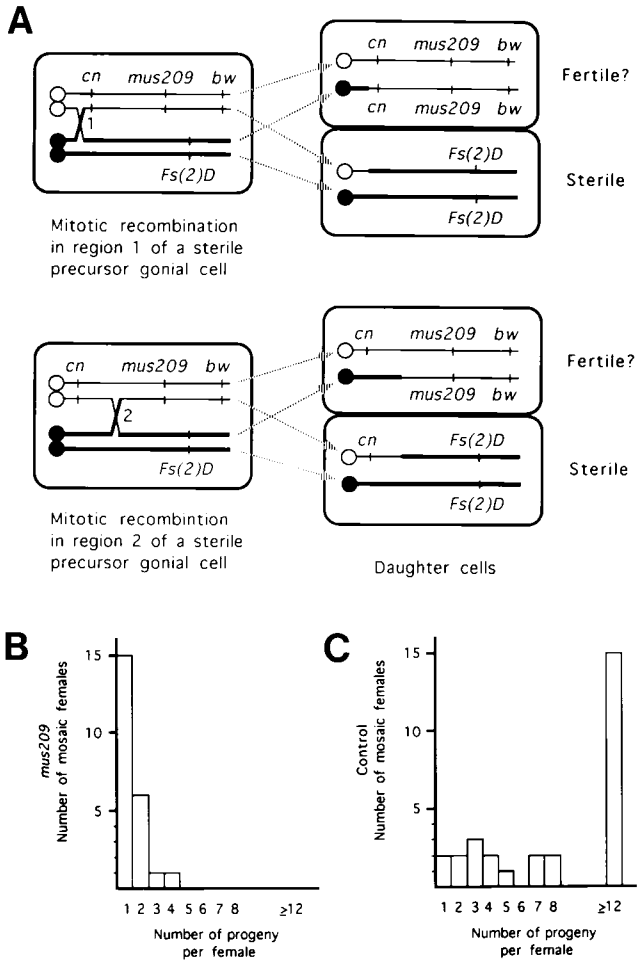

Figure 2.—(A) Diagram of the procedure used to induce homozygous germ-line clones in females (see text for details). Germ lines that carry the dominant female sterile mutation *Fs(2)D* do not produce eggs. Arrows indicate segregation of centromeres. (B) Histogram showing the fecundity (number of viable adult progeny per female) of X-ray-induced "fertile" *mus209*^{B1} germ lines. (C) Histogram showing the fecundity of X-ray-induced wild-type germ lines.

each, 4 was the maximum number of offspring produced by a *mus209*^{B1}/*Fs(2)D* mosaic female. These data establish that a defect in cell proliferation in the germ line is a significant causative factor in the sterility of

TABLE 1

Induction of *mus209*^{B1} homozygous clones in the female germ line: analysis of fertility

Female genotype	X-ray dose (Gy)	No. of females tested	No. of fertile females	Frequency of induced fertility (%)
mus209^{B1}/*Fs(2)D*	8.5	2713	23	0.9
	0	446	0	0.0
mus209^{+}/*Fs(2)D*	8.5	513	29	5.7
	0	304	0	0.0

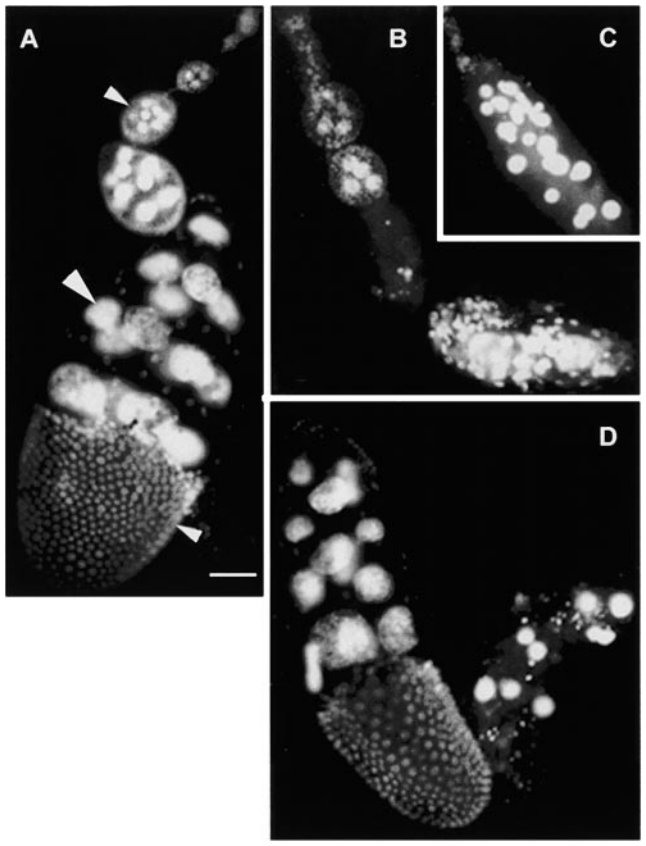

Figure 3.—Partial rescue of oogenesis in *mus209*^{B1}/*mus209*^{2735} females. (A) A phenotypcially wild-type ovariole from a *mus209*^{B1}/+ adult showing four egg chambers at successive stages of development (culminating at stage 10B). Approximately 15 such ovarioles make up a wild-type ovary. The large arrow points to a nurse cell nucleus; the small arrows to follicle cell nuclei. Bar, 50 μm. (B–D) Examples of ovarioles and egg chambers from PCNA-deficient *mus209*^{B1}/*mus209*^{2735} females. Most egg chambers display defects in follicle cell proliferation and/or migration (B), sometimes resulting in fusion of adjacent egg chambers (not shown). The egg chamber in C has approximately double the number of nurse cell nulcei and may have resulted from such a fusion or from an extra round of cystocyte division. Phenotypically normal egg chambers can be produced by *mus209*^{B1}/*mus209*^{2735} females (*e.g.*, left egg chamber in D). These can be found anterior or posterior to an abnormal egg chamber in a single ovariole.

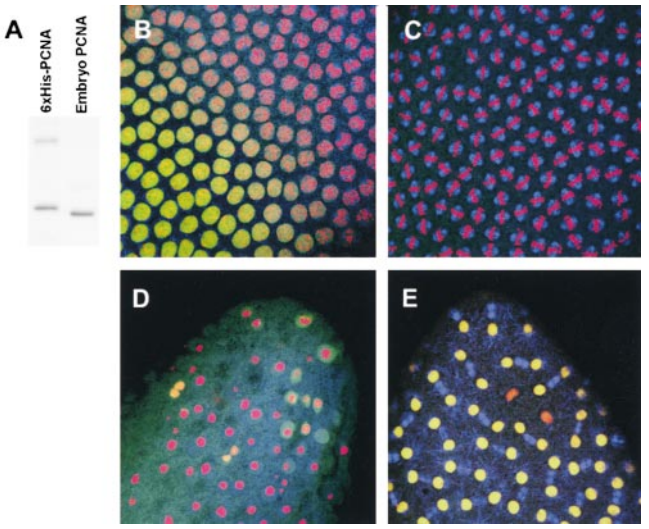

Figure 4.—Nuclear divisions in syncytial embryos derived from *mus209*^{B1}/*mus209*^{2735} females. (A) Characterization of new anti-Drosophila PCNA antiserum by SDS-PAGE and immunoblotting. (Left) Bacterially expressed Drosophila PCNA carrying an N-terminal histidine tag (6xHis-PCNA) and purified by metal affinity chromatography (see materials and methods). Band corresponds to $M_r = 34 \times 10^3$. (Right) Drosophila protein extract from 0- to 2-hr-old embryos. Band corresponds to $M_r = 32 \times 10^3$. (B–E) Laser scanning confocal microscopic images of syncytial-stage embryos derived from *mus209*^{B1}/*mus209*^{2735} females mated to wild-type (*Oregon-R*) males. Green, PCNA; red, DNA; blue, tubulin. (B) Progression of a mitotic wave in a phenotypically normal embryo. Interphase nuclei at bottom left are stained positive for PCNA; PCNA staining disappears from chromatin as prophase ensues (center and top right). (C) Phenotypically normal metaphase figures. PCNA is dispersed in the common cytoplasm. (D) Grossly abnormal embryo showing uneven distribution of nuclei and aberrant PCNA and tubulin staining. (E) More normal embryo showing telophase nuclei stained positive for PCNA. Note "fall-out" sister nuclei (orange) that are "PCNA negative."

mus209^{B1} females, although as there is some fertility in the recombinants, we cannot rule out the possibility that the wild-type soma might have some rescuing ability (see discussion).

Fertility is partially restored in *mus209*^{B1}/*mus209*^{2735} heteroallelic females: The partial fertility of heteroallelic *mus209*^{B1}/*mus209*^{2735} females is an intriguing example of interallelic complementation because it indicates that a trimer composed of different mutant subunits (*i.e.*, B1-B1-2735 and/or B1-2735-2735) must function more effectively than either mutant homotrimer, at least in oogenesis. To determine the extent to which these partially complementing PCNA monomers restore normal function to the *mus209*^{B1}/*mus209*^{2735} ovary, we studied oogenesis within such mutant females, with the syncytial embryonic development of their progeny. Whereas the ovarioles from heterozygous *mus209*^{B1}/+ females appear wild type (Figure 3A), those from *mus209*^{B1}/*mus209*^{2735} females develop further than their homozygous mutant counterparts and yet still show a variety of developmental defects. These can include defects in follicle cell proliferation or migration (Figure 3, B–D). In addition, egg chambers are formed that contain approximately double the normal number of nurse cells (Figure 3C). This could be explained either by the occurrence of an extra round of mitosis before the onset of endoreduplication or by fusion of egg chambers. Some egg chambers appear normal, however (Figure 3D, left), thus explaining the ability of flies of this genotype to produce some offspring.

The syncytial embryos derived from *mus209*^{B1}/*mus209*^{2735} mothers likewise show a range of defects. A total of 10–20% appear wild type and show mitotic gradients in which PCNA is present in interphase nuclei

TABLE 2

Meiotic recombination on chromosome 2 in *mus209*^{B1} / *mus209*^{2735} females

Recombinant class	Number of progeny: Maternal genotype: *mus209*^{B1} / *mus209*^{2735}	+ / +
Noncrossovers	2369	2479
Single crossovers		
Region 1[a]	339	498
2	1050	1497
3	361	282
4	66	35
Double crossovers		
1, 2	33	33
1, 3	22	25
1, 4	13	10
2, 3	35	29
2, 4	16	27
3, 4	18	4
Triple crossovers		
1–3	1	2
1, 2, 4	1	0
2–4	2	0
	N = 4326	*N* = 4921

[a] Region 1, *al-dp*; region 2, *dp-b*; region 3, *b-pr*; region 4, *pr-cn* (includes the centromere).

TABLE 3

Comparison of meiotic map intervals in *mus209* mutant and control females

Crossover region[a]	Map length (cM): *mus209*^{B1} / *mus209*^{2735}	+ / +	Ratio of mutant map to control map
1	9.5	11.5	0.8
2	26.3	32.3	0.8
3	10.2	7.0	1.5
4	2.7	1.5	1.8
1–4	48.7	52.3	

[a] Crossover regions are defined in Table 2.

(Figure 4B), disappears at prometaphase (Figure 4B), and is absent at metaphase (Figure 4C). Others show varying degrees of abnormality in the distribution of nuclei. Embryos with highly irregular nuclei often appear to be arrested in cell cycle progression, with the nuclei showing no staining of PCNA (Figure 4D). In others, aberrant nuclear division leads to nuclear "fallout" from cortex, as has been described previously (Sullivan *et al.* 1993). In this case, only those nuclei that remain undergoing rounds of replication and division at the cortex continue to have detectable PCNA within them (Figure 4E).

Meiotic crossing over occurs in *mus209*^{B1} / *mus209*^{2735} females: We have shown previously that *mus209*$^{+}$ function is required for DSB repair, and so we wished to determine whether there might be a requirement for PCNA during meiotic exchange in oogenesis. We therefore set out to determine whether meiotic recombination frequencies were affected in the germ line of the partially fertile *mus209*^{B1} / *mus209*^{2735} females. Recombination was monitored using a multiply mutant chromosome whose markers (*al*, *dp*, *b*, *pr*, and *cn*) span the entire left arm and centromeric region of chromosome 2. Heterozygous *al dp b pr cn mus209*^{2735} / + + + + + *mus209*^{B1} females were crossed to *al dp b pr cn* homozygous males, and their adult progeny were scored for the five mutant markers (Tables 2 and 3). The overall level of recombination, as measured by genetic map length, is reduced in *mus209*^{B1} / *mus209*^{2735} compared to wild type, but only marginally so (48.7 *vs.* 52.3 cM; Table 3). However, when each crossover interval is examined separately it can be seen that while the proportion of distal exchange events (*i.e.*, in regions 1 and 2) is reduced, the proportion of centromere-proximal exchanges (*i.e.*, those in regions 3 and 4) is actually increased (Table 3). A similar pattern of reapportioned exchanges is a characteristic of so-called "precondition" meiotic mutants of Drosophila, the effect of which is to render the genetic map of the chromosome more reflective of actual physical distance (Baker and Carpenter 1972).

Partial reversal of a DNA repair defect in *mus209*^{B1} / *mus209*^{2735} heterozygotes: The failure of *mus209*^{B1} homozygotes to undertake repair of DNA DSBs is evident during *P*-element transposition. In this process, transposase-mediated excision of an element leaves behind a DSB, which results in lethality when not repaired (Henderson and Glover 1998). The assay for DSB repair (Banga *et al.* 1991) involves incorporating a *mus209* mutant into an active transposition system comprising an *in vitro*-modified *P* element, Δ*2-3(68C)*, which serves as a source of transposase in somatic cells, and target *P* elements inserted at the X-linked locus *sn* (*singed*). The allele that we used, *sn*^{w} (*singed-weak*), is actually a double insertion mutation consisting of two internally deleted *P* elements (Roiha *et al.* 1988). Since neither *P* element encodes a functional transposase, *sn*^{w} is normally stable. However, when crossed to a transposase-producing line, such as Δ*2-3(68C)*, one or the other *P* element (Roiha *et al.* 1988) is excised at a high frequency in cells of the F_1 progeny, generating a site-specific DSB. Repair proficiency can be expressed in terms of survival. We showed previously that transposase-producing *sn*^{w} / *Y; mus209*^{B1} / *mus209*^{B1} males and *sn*^{w} / +; *mus209*^{B1} / *mus209*^{B1} females fail to undertake DSB repair and that unrepaired DSBs can lead to chromosomal breaks (Henderson and Glover 1998). Particularly striking is the dominant nature of this lethality in females, which were killed despite having had a wild-type X chromosome in addition to the *sn*^{w}-bearing homolog. We have extended this analysis to *mus209*^{2735} homozygous females

TABLE 4

Analysis of DSB repair in *mus209* homozygous and heteroallelic mutants

	Genotype of progeny	No. of progeny	Relative viability
Cross 1	+ / +; *mus209*^{2735} / *CyO*; Δ*2-3* / Δ*2-3* × *sn*^{w} / *Y*; *mus209*^{2735} / *CyO*		
	a + / *sn*^{w}; *mus209*^{2735} / *mus209*^{2735}; Δ*2-3* / +	1	0.02
	b + / *sn*^{w}; *mus209*^{2735} / *CyO*; Δ*2-3* / +	79	
	c + / *Y*; *mus209*^{2735} / *mus209*^{2735}; Δ*2-3* / +	45	1.08
	d + / *Y*; *mus209*^{2735} / *CyO*; Δ*2-3* / +	83	
Cross 2	+ / +; *mus209*^{B1} / *CyO*; Δ*2-3* / Δ*2-3* × *sn*^{w} / *Y*; *mus209*^{B1} / *CyO*		
	e + / *sn*^{w}; *mus209*^{B1} / *mus209*^{B1}; Δ*2-3* / +	2	0.02
	f + / *sn*^{w}; *mus209*^{B1} / *CyO*; Δ*2-3* / +	180	
	g + / *Y*; *mus209*^{B1} / *mus209*^{B1}; Δ*2-3* / +	62	0.80
	h + / *Y*; *mus209*^{B1} / *CyO*; Δ*2-3* / +	154	
Cross 3	+ / +; *mus209*^{B1} / *CyO*; Δ*2-3* / Δ*2-3* × *sn*^{w} / *Y*; *mus209*^{2735} / *CyO*		
	i + / *sn*^{w}; *mus209*^{B1} / *mus209*^{2735}; Δ*2-3* / +	64	0.65
	j + / *sn*^{w}; *mus209*$^{B1 \text{ or } 2735}$ / *CyO*; Δ*2-3* / +	197	
	k + / *Y*; *mus209*^{B1} / *mus209*^{2735}; Δ*2-3* / +	109	1.08
	l + / *Y*; *mus209*$^{B1 \text{ or } 2735}$ / *CyO*; Δ*2-3* / +	201	

The *CyO* balancer chromosome carries the dominant marker *Cy* and a wild-type allele of *mus209*. Relative viability is the ratio of *mus209* homozygous or heteroallelic mutant (non-Cy) to their *mus209* / *CyO* (Cy) same-sex siblings in each cross. The values obtained were multiplied by 2 since each cross was expected to produce half as many non-Cy as Cy offspring (the *CyO* / *CyO* genotype is inviable).

and find that when transposase is expressed in the presence of the *sn*^{w} target, there are few viable organisms (Table 4, cross 1, genotype a). In contrast to *mus209*^{B1} and *mus209*^{2735} homozygotes, transposase-producing *sn*^{w} / +; *mus209*^{B1} / *mus209*^{2735} females exhibit significant survival (Table 4, cross 3, genotype i), indicating that the mutant PCNA subunits partially complement one another to allow DSB repair to occur in somatic cells. Therefore, *mus209*^{B1} and *mus209*^{2735} complement not only in allowing more extensive ovarian development to partially correct sterility, but also for the DSB repair deficiency.

Relationships between the structure and function of PCNA revealed in cold-sensitive and nonconditional lethal *mus209* mutants: We have determined the mutated amino acids in four additional *mus209* mutants—a cold-sensitive lethal allele (*mus209*$^{D\text{-}1368}$) and three nonconditional lethal alleles (*mus209*^{36}, *mus209*^{157}, and *mus209*^{775})—and modeled these residues on the three-dimensional structure of PCNA as done for *mus209*^{B1} and *mus209*^{2735}. The effects of the four mutations are readily explainable in the context of the known molecular structure of PCNA. This is in contrast to the complementation that occurs between *mus209*^{B1} and *mus209*^{2735}, an interaction not easily explained solely in terms of the trimer model of the protein (see discussion).

The cold-sensitive mutant *mus209*$^{D\text{-}1368}$ is the weakest allele in our collection, being only moderately sensitive to mutagens and exhibiting some survival at its restrictive temperature. However, like its heat-sensitive counterparts, it is female sterile (Table 5). *mus209*$^{D\text{-}1368}$ carries a glutamine-to-lysine substitution at the solvent-exposed N-terminal residue 3 (E3K; Figure 5A). Given the distance of this residue from both interdomain and intermolecular boundaries, E3K is not expected to interfere with either the folding of the PCNA monomer or its ability to form trimers. Rather, E3 is one element of what appears to be a conserved surface patch of predominantly charged residues (E3, R5, R61, T89, and K91 in Figure 5A). We suggest that this patch is a site of interaction between PCNA and some other protein(s), possibly pol δ (Arroyo *et al.* 1996).

The three nonconditional lethal *mus209* mutants we have studied share the phenotype of early developmental lethality (Table 5). The first of these, *mus209*^{36}, carries a valine-to-aspartate substitution at residue 48 (V48D) in β strand D_1 (βD_1; Figure 5B). This highly conserved amino acid lies at the core of the PCNA monomer at the interface of its two domains. Such a substitution of an internal hydrophobic for a charged residue is expected to alter the overall conformation of the monomer, most probably by disrupting its correct folding. These molecular data would be consistent with the severe phenotype of *mus209*^{36}, a probable PCNA-null mutant. That such a mutant would begin to develop at all may be explained by the perdurance of wild-type PCNA deposited into the egg by the heterozygous mother. A second lethal allele, *mus209*^{157}, carries a tyrosine-to-asparagine substitution at residue 249 (Y249N), also located at the core of the monomer (Figure 5B). Indeed, although they are separated by 200 amino acids on the primary structure of PCNA and reside in different

topological domains, Y249 and V48 lie apposed in antiparallel β strands at the interdomain interface. These two lethal mutations thus confirm the importance of this structural element for PCNA function.

The third lethal mutant, *mus209*^{775}, has a valine-to-aspartate substitution at residue 99 (V99D) near the intermolecular interface (Figure 5C). This interface is structurally similar to the interdomain interface of the monomer in several respects: both feature interactions between antiparallel β strands, consisting of eight main-chain hydrogen bonds; each interface bisects an extensive, contiguous β sheet; and both interfaces have hydrophobic interiors (Krishna *et al.* 1994). It is possible that V99D causes a localized perturbation of βH_1 at the intermolecular interface, disrupting trimerization. Single-amino-acid changes in βI_1 adjacent to V99 (at residues 114 and 115 in Figure 5C) have been shown to disrupt trimerization of PCNA *in vitro* (Ayyagari *et al.* 1995; Jónsson *et al.* 1995). Alternatively, V99D may alter the general folding of the monomer to produce a completely nonfunctional protein. Either effect would be consistent with the severe phenotype of *mus209*^{775}.

DISCUSSION

Heat-sensitive PCNA mutants have not been isolated in any other organism despite efforts to recover them (Aaygari *et al.* 1995; Amin and Holm 1996; Arroyo *et al.* 1996). The two heat-sensitive mutants, *mus209*^{B1} and *mus209*^{2735}, that we describe in this study are of particular interest not only because the mutated amino acids are found at similar positions in the conserved 3D structure, but also because the two mutations show interallelic complementation.

The developmental stage most affected by each of these mutations is oogenesis, a process that places a large demand upon the DNA replicative machinery, in the cycles of endoreduplication that are undertaken by both the follicle cells, derived from the soma, and the nurse cells derived from the germ line. Ovaries in *mus209* mutant adults are underdeveloped and devoid of mature eggs. In these respects, *mus209* mutants resemble members of a class of female-sterile mutants described by Schüpbach and Wieschaus (1991), the most severe of which are characterized by having small, underdeveloped ovaries with few or no germ cells. Such a phenotype is expected if stem cells or cystocytes fail to divide, or if stem cell precursors fail to populate the developing gonad during embryonic, larval, or pupal stages of development (Schüpbach and Wieschaus 1991).

Two pieces of evidence point toward a limitation of the germ line to proliferate as a result of these mutations. First, we see drastically reduced numbers of cells expressing the *ovo-lacZ* reporter specific for the germ line. Moreover, using the dominant female sterile technique to generate homozygous *mus209*^{B1} mutant germ cells in a background of heterozygous (wild-type phenotype) soma, we demonstrate a profound effect of the *mus209*^{B1} mutation upon fertility. However, although the fertility that is induced by X-ray-mediated recombination in the *mus209*^{B1}/*Fs(2)D* mosaics was substantially reduced relative to the control, it was not completely abolished; 23 *mus209*^{B1}/*Fs(2)D* females produced germline clones that gave rise to a few viable offspring (usually one or two). What might account for this partial fertility when *mus209*^{B1} homozygotes are completely sterile? One possibility is that after mitotic recombination and cytokinesis, wild-type PCNA provided by the heterozygous mother cell perdures in the newly formed *mus209*^{B1} daughter cell (see Perrimon *et al.* 1984). This might provide sufficient PCNA for the few cell division cycles necessary to produce one or two eggs. A second factor that may contribute to the difference in fertility between

TABLE 5

Summary of properties of *mus209* mutants

Allele	Mutation	Lethal class	Lethal phase of hemizygote[a]	Other phenotypes[b]
mus209^{B1}	P140L	Heat sensitive	Pupal	mus, fs, su(var)
mus209^{2735}	V195E	Heat sensitive	Pupal	mus, fs, su(var)
mus209$^{D\text{-}1368}$	E3K	Cold sensitive[c]	Pupal	mus, fs, su(var)
mus209^{36}	V48D	Nonconditional	Embryo/first instar[d,e]	
mus209^{157}	Y249N	Nonconditional	Embryo/first instar[d]	
mus209^{775}	V99D	Nonconditional	Embryo/first instar	

[a] Lethal phases were determined for animals heterozygous for the indicated *mus209* allele and the deficiency chromosome *Df(2R)173* (paternally derived), which deletes *mus209*$^{+}$.

[b] mus, mutagen sensitive; fs, agametic female sterile; su(var), suppressor of position-effect variegation.

[c] *mus209*$^{D\text{-}1368}$ homozygotes have been observed to develop to adults at all temperatures routinely used to culture flies (18–29°). However, their survival was found to be poorest at 18°.

[d] *mus209*^{36}/*mus209*^{157} heteroallelic animals also die as embryos/first instar larvae.

[e] Hemizygous mutant animals can survive to later stages when parents and progeny are cultured on enriched medium (Y. Inoue, personal communication).

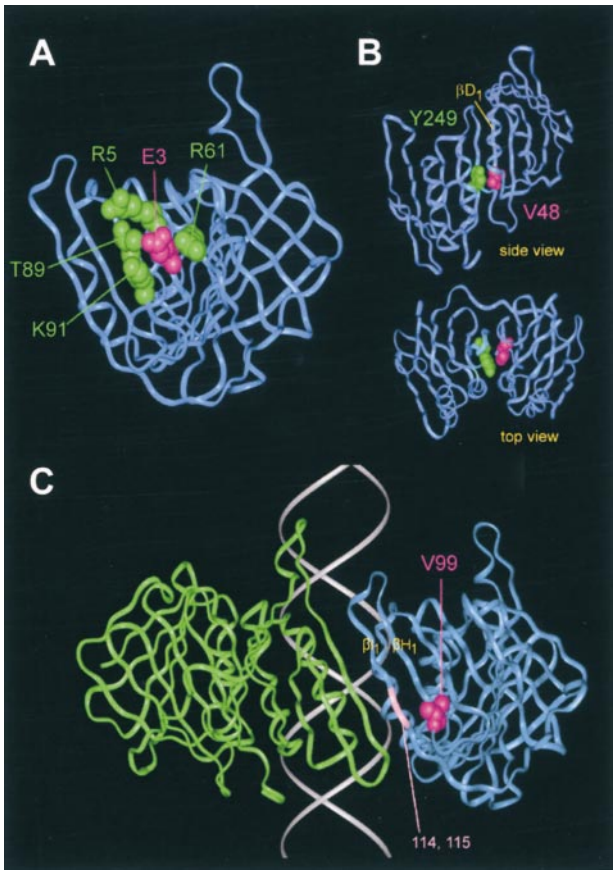

Figure 5.—Computer-generated models of PCNA showing the positions of residues mutated in cold-sensitive and nonconditional lethal alleles of *mus209*. (A) Model of a PCNA monomer showing the position of the amino-terminal residue E3 (crimson) mutated in the cold-sensitive mutant *mus209*$^{D\text{-}1368}$. E3 and four neighboring residues (R5, R61, T89, and K91, colored green) form a conserved surface patch on the monomer, a possible site of contact between PCNA and some other protein. The orientation of this monomer in relation to trimeric PCNA can be visualized by comparing it to the structure in C. (B) Models of a monomer showing the positions of the residues mutated in the nonconditional lethal alleles *mus209*^{36} (V48, crimson) and *mus209*^{157} (Y249, green). Both mutations affect conserved residues at the interdomain interface at the core of the monomer. β strand D_1 is labeled. (C) Model of PCNA on DNA showing an interface between two monomers, colored green and blue. For clarity, the third PCNA subunit is not shown. The position of the amino acid residue mutated in the nonconditional lethal allele *mus209*^{775} is indicated (V99). βH_1 and βI_1 denote β strands at the intermolecular interface. Mutation of either residue 114 or 115 (colored pink; Y114A in human PCNA and S115P in yeast PCNA) can result in defective trimerization.

mus209^{B1}/*Fs(2)D* mosaics and *mus209*^{B1} homozygotes is the genotype of their respective ovarian soma; that of the former is functionally wild type and that of the latter is mutant (*i.e.*, *mus209*^{B1}). The combined effect of mutant germ line and mutant soma is likely to have more dire consequences for fertility than when the germ line alone is mutant.

Heteroallelic *mus209*^{B1}/*mus209*^{2735} females also produce some egg chambers that have normal appearance, but the complementation is far from complete and abnormal egg chambers can also be seen. These may show defects in either or both the development of the somatic follicle cells or the germ line nurse cells, thus supporting a requirement for PCNA in both of these cell types, as inferred from the germ-line clonal analysis. Some egg chambers have up to 30 nurse cells, suggesting that there has been an extra round of cell division before the onset of the endoreduplication cycles. It is also possible that egg chambers have undergone fusion, facilitated by the incomplete development of the associated follicle cells. Nevertheless, the extent of interallelic complementation is sufficient to produce a considerable number of eggs, although the majority of these do not hatch (Henderson *et al.* 1994). Varying numbers of nuclei appear to drop out of the division cycles during the syncytial stages and, in constrast to cycling interphase nuclei, no longer contain detectable PCNA. These generally appear to lose contact with the cytoskeletal elements at the cortex of the embryo and fall into the interior, as has been described for other cases of defective nuclear division (Sullivan *et al.* 1993). It would seem that only a fraction of *mus209*^{B1}/*mus209*^{2735}-derived eggs have sufficient PCNA activity to meet the heavy demand imposed by embryogenesis on the DNA synthesis machinery. Cleavage stage nuclei in Drosophila embryos replicate their genomes in only 3–4 min (Rabinowitz 1941), one of the shortest durations of S phase known for any organism.

The partial fertility of the *mus209*^{B1}/*mus209*^{2735} combination has also allowed us to test the requirement for PCNA in meiotic recombination. We observed small differences in map distances between this mutant combination and wild type. The reapportionment of exchange events is graded along the chromosome arm; recombination is decreased distally but is increased for intervals closer to the centromere. Second, chiasma interference is decreased in the distal regions (data not shown). Each of these features is characteristic of the "precondition" class of mutants defective in functions thought to establish the positions of recombination nodules (Sandler *et al.* 1968), sites of DNA repair synthesis (Carpenter 1981). In addition to these effects upon exchange, tetrad analysis (Weinstein 1936) indicates that the proportion of nonexchange (E_0) tetrads is increased in *mus209*^{B1}/*mus209*^{2735} compared to wild type, primarily at the expense of single-exchange tetrads (data not shown). Consistent with an increase in E_0, the frequency of nondisjunction is increased by at least 10-fold in *mus209*^{B1}/*mus209*^{2735} compared to wild type, as measured for the X chromosome. (We have observed frequencies of X chromosome nondisjunction of 1.2 and 2.4%.)

Interallelic complementation between *mus209*^{B1} and *mus209*^{2735} is evident not only in oogenesis, but also in the partial ability to rescue lethality resulting from fail-

ure to repair DSBs induced by *P*-element excision. Females of the genotype $sn^{w}/+; mus209^{B1}/mus209^{B1}$ fail to undertake DSB repair and this can lead to chromosomal breakage and dominant lethality (Henderson and Glover 1998). This lethality, which can also be seen in homozygous $mus209^{2735}$ females, is reduced in the $mus209^{B1}/mus209^{2735}$ heteroallelic combination.

Taken together, our data indicate that a PCNA trimer composed of two different mutant forms of monomer may function better than either mutant homotrimer. Moreover, the interallelic complementation that we observe between $mus209^{B1}$ and $mus209^{2735}$ is novel in that the affected residues lie at adjacent sites in the three-dimensional structure of the monomer. The evidence that the mutations are in the same functional domain, although not absolute, is compelling: the C_α atoms of the affected residues P140 and V195 are 7.25 Å apart, and the distance between C_δ of P140 and C_β of V195, the closest approach, is 4.8 Å; the side chains of both residues are in the same solvent-inaccessible environment; the mutations result in the same range of temperature sensitivity; they confer identical mutant phenotypes measured by either mutagen sensitivity, degree of suppression of position-effect variegation, or female sterility.

How, then, might this mutual correction occur? A conventional explanation of interallelic complementation is that the protein possesses two (or more) autonomous functional domains, and that complementation occurs because each mutant polypeptide retains a function that the other lacks (*e.g.*, Rawls and Fristrom 1975). Since the mutations in $mus209^{B1}$ and $mus209^{2735}$ appear to reside in the same functional domain, this model does not explain the interallelic complementation. The second conventional explanation of interallelic complementation is that the native protein is composed of two or more identical subunits. In such a multimeric protein, *e.g.*, a dimer, conformational changes in the two mutant forms of monomer are imagined to offset each other to allow the "heterodimer" to function better than either mutant homodimer. However, this model also seems inadequate to explain the complementation between $mus209^{B1}$ and $mus209^{2735}$. For example, in a B1-B1-2735 or B1-2735-2735 trimer, two of the monomers are of the same mutant form, thereby precluding a mutually correcting interaction between those two subunits. Furthermore, given the locations of the two mutated residues on the structure of PCNA, any offsetting conformational changes would have to be long range, across the trimer (see Figure 1B).

An alternative to these conventional views of interallelic complementation is that correction is mediated through some other protein or protein complex that interacts simultaneously with two or all three subunits of the PCNA trimer, and whose binding possibly involves the D_2E_2 loops. These loops on the "heteromeric" mutant trimer might have a conformation more closely resembling wild type compared to either mutant homotrimer and, therefore, have greater affinity for the interacting molecule (Figure 6A). A weakness of this model is that no molecule has yet been found to interact with the D_2E_2 loop.

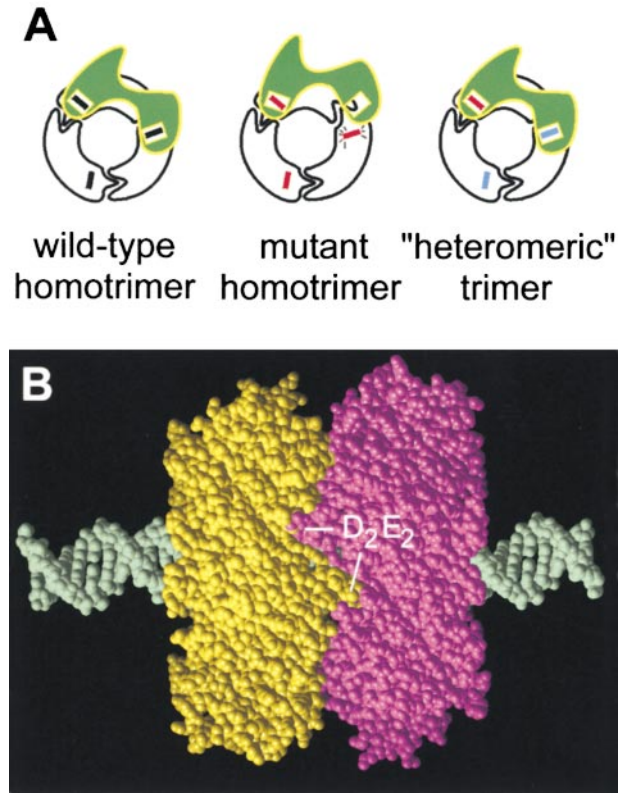

Figure 6.—Models for interallelic complementation. (A) In this model, PCNA is seen to interact with some other intermediate molecule that has two binding sites that differ in affinities. One mutant (red box, representing a D_2E_2 loop) permits interaction of PCNA with one but not the other binding site. The second mutant form (blue box, also representing a D_2E_2 loop) retains affinity for the second but not the first site, thus permitting formation of functional heterotrimer. (B) In this model, native PCNA is assumed to be a dimer of trimers. Trimeric PCNA molecules are proposed to interact "back-to-back" with the D_2E_2 loops (labeled) of one face interdigitated with those of the other face. One trimer is colored yellow and the other magenta.

A second alternative model would be if two PCNA trimers were to interact "back to back," with the D_2E_2 loops as points of contact or interdigitation. This could explain why so far no molecule has been found to interact with the backside of PCNA. All of the PCNA-binding proteins that have been described interact either with the interconnector loop or its front face. It is possible to construct a back-to-back model of PCNA trimers by a process of interactive computer graphics and energy minimization giving satisfactory steric interactions and interdigitation of surface loops (Figure 6B). However, given the size and complexity of this modeled interface, assessment of the validity of this model is difficult, and so it must be regarded as highly speculative. The at-

traction of this model is that it could explain the mutant interactions described in this article, and also provide a solution to some of the problems associated with the directionality implicit in the trimeric structure. A back-to-back PCNA hexamer could operate in either direction along DNA.

We are grateful to Ken Burtis, Cayetano Gonzalez, Scott Hawley, John Kiger, Hiroyuki Ohkura, Terry Orr-Weaver, Alastair Philp, Helen White-Cooper, and Rochele Yamamoto for their helpful discussions and critical comments on various aspects of this work. We thank Fiona Cullen and Sabine Corbach for technical assistance, Trudi Schüpbach for providing *Fs(2)D* and advice, and Cathy Salles for the *ovo-lacZ* reporter line. This work was supported by the Cancer Research Campaign.

Note added in proof: In an article by Maga *et al.* (G. Maga, Z. O. Jónsson, M. Stucki, S. Spadari and U. Hübscher, 1999, Dual mode of interaction of DNA polymerase ε with proliferating cell nuclear antigen in primer binding and DNA synthesis. J. Mol. Biol. **285:** 259–267) that has recently come to our attention, biochemical data that the authors have interpreted as indicating that DNA polymerase ε can interact with both the front and back of the PCNA trimer are presented. We point out that their data could also be explained in terms of the hexamer model of PCNA that we propose here.

LITERATURE CITED

Amin, N. S., and C. Holm, 1996 *In vivo* analysis reveals the interdomain region of the yeast proliferating cell nuclear antigen is important for DNA replication and DNA repair. Genetics **144:** 479–493.

Arroyo, M. P., and T. S.-F. Wang, 1998 Mutant PCNA alleles are associated with cdc phenotypes and sensitivity to DNA damage in fission yeast. Mol. Gen. Genet. **257:** 505–518.

Arroyo, M. P., K. M. Downey, A. G. So and T. S.-F. Wang, 1996 *Schizosaccharomyces pombe* proliferating cell nuclear antigen mutations affect DNA polymerase δ processivity. J. Biol. Chem. **271:** 15971–15980.

Ausubel, F. M., R. Brent, R. E. Kingston, D. D. Moore, J. G. Seidman *et al.*, 1998 *Current Protocols in Molecular Biology*. John Wiley & Sons, New York.

Ayyagari, R., K. J. Impellizzeri, B. L. Yoder, S. L. Gary and P. M. J. Burgers, 1995 A mutational analysis of the yeast proliferating cell nuclear antigen indicates distinct roles in DNA replication and DNA repair. Mol. Cell. Biol. **15:** 4420–4429.

Baker, B. S., and A. T. C. Carpenter, 1972 Genetic analysis of sex chromosomal meiotic mutants in *Drosophila melanogaster*. Genetics **71:** 255–286.

Banga, S. S., B. T. Bloomquist, R. K. Brodberg, Q. N. Pye, D. C. Larrivee *et al.*, 1986 Cytogenetic characterization of the 4BC region on the X chromosome of *Drosophila melanogaster*: localization of the *mei-9*, *norpA* and *omb* genes. Chromosoma **93:** 341–346.

Banga, S. S., A. Velazquez and J. B. Boyd, 1991 P transposition in Drosophila provides a new tool for analyzing postreplication repair and double-strand break repair. Mutat. Res. **255:** 79–88.

Bellen, H. J., and J. A. Kiger, 1988 Maternal effects of general and regional specificity on embryos of *Drosophila melanogaster* caused by *dunce* and *rutabaga* mutant combinations. Roux's Arch. Dev. Biol. **197:** 258–268.

Carpenter, A. T. C., 1981 EM autoradiographic evidence that DNA synthesis occurs at recombination nodules during meiosis in *Drosophila melanogaster* females. Chromosoma **83:** 59–80.

Chuang, L. S., H. I. Ian, T. W. Koh, H. H. Ng, G. Xu *et al.*, 1997 Human DNA-(cytosine-5) methyltransferase-PCNA complex as a target for $p21^{WAF1}$. Science **277:** 1996–2000.

FlyBase, 1999 The FlyBase database of the *Drosophila* Genome Projects and community literature. Nucleic Acids Res. **27:** 85–88 (available from http://flybase.bio.indiana.edu/).

Fotedar, R., R. Mossi, P. Fitzgerald, T. Rousselle, G. Maga *et al.*, 1996 A conserved domain of the large subunit of replication factor C binds PCNA and acts like a dominant negative inhibitor of DNA replication in mammalian cells. EMBO J. **15:** 4423–4433.

Frosina, G., P. Fortini, O. Rossi, F. Carrozzino, G. Raspaglio *et al.*, 1996 Two pathways for base excision repair in mammalian cells. J. Biol. Chem. **271:** 9573–9578.

Fukuda, K., H. Morioka, S. Imajou, S. Ikeda, E. Ohtsuka *et al.*, 1995 Structure-function relationships of the eukaryotic DNA replication factor, proliferating cell nuclear antigen. J. Biol. Chem. **270:** 22527–22534.

Gary, R., D. L. Ludwig, H. L. Cornelius, M. A. MacInnes and M. S. Park, 1997 The DNA repair endonuclease XPG binds to proliferating cell nuclear antigen (PCNA) and shares sequence elements with the PCNA-binding regions of FEN-1 and cyclin-dependent kinase inhibitor p21. J. Biol. Chem. **272:** 24522–24529.

Gatti, M., and M. L. Goldberg, 1991 Mutations affecting cell division in *Drosophila*. Methods Cell Biol. **35:** 543–586.

Gu, L., Y. Hong, S. McCulloch, H. Watanabe and G.-M. Li, 1998 ATP-dependent interaction of human mismatch repair proteins and a dual role of PCNA in mismatch repair. Nucleic Acids Res. **26:** 1173–1178.

Gulbis, J. M., Z. Kelman, J. Hurwitz, M. O'Donnell and J. Kuriyan, 1996 Structure of the C-terminal region of $p21^{WAF1/CIP1}$ complexed with human PCNA. Cell **87:** 297–306.

Harlow, E., and D. P. Lane, 1988 *Antibodies: A Laboratory Manual*. Cold Spring Harbor Laboratory Press, Cold Spring Harbor, NY.

Henderson, D. S., 1999 Use of P element transposons to study DNA double-strand break repair in *Drosophila melanogaster*, pp. 417–424 in *DNA Repair Protocols: Eukaryotic Systems*, edited by D. S. Henderson. Humana Press, Totowa, NJ.

Henderson, D. S., and D. M. Glover, 1998 Chromosome fragmentation resulting from an inability to repair transposase-induced DNA double-strand breaks in PCNA mutants of *Drosophila*. Mutagenesis **13:** 57–60.

Henderson, D. S., S. S. Banga, T. A. Grigliatti and J. B. Boyd, 1994 Mutagen sensitivity and suppression of position-effect variegation result from mutations in *mus209*, the *Drosophila* gene encoding PCNA. EMBO J. **13:** 1450–1459.

Holmes, A. M., and J. E. Haber, 1999 Double-strand break repair in yeast requires both leading and lagging strand DNA polymerases. Cell **96:** 415–424.

Johnson, R. E., G. K. Kovvali, S. N. Guzder, N. S. Amin, C. Holm *et al.*, 1996 Evidence for involvement of yeast proliferating cell nuclear antigen in DNA mismatch repair. J. Biol. Chem. **271:** 27987–27990.

Jónsson, Z. O., V. N. Podust, L. M. Podust and U. Hübscher, 1995 Tyrosine 114 is essential for the trimeric structure and the functional activities of human proliferating cell nuclear antigen. EMBO J. **14:** 5745–5751.

Jónsson, Z. O., R. Hindges and U. Hübscher, 1998 Regulation of DNA replication and repair proteins through interaction with the front side of proliferating cell nuclear antigen. EMBO J. **17:** 2412–2425.

Kelman, Z., 1997 PCNA: structure, function and interactions. Oncogene **14:** 629–640.

King, R. C., 1970 *Ovarian Development in Drosophila melanogaster*. Academic Press, New York.

Klungland, A., and T. Lindahl, 1997 Second pathway for completion of human DNA base excision-repair: reconstruction with purified proteins and requirement for DNase IV (FEN1). EMBO J. **16:** 3341–3348.

Krishna, T. S. R., X.-P. Kong, S. Gary, P. M. J. Burgers and J. Kuriyan, 1994 Crystal structure of the eukaryotic DNA polymerase processivity factor PCNA. Cell **79:** 1233–1243.

Lindsley, D. L., and G. G. Zimm, 1992 *The Genome of Drosophila melanogaster*. Academic Press, San Diego.

Matsumoto, Y., K. Kim and D. F. Bogenhagen, 1994 Proliferating cell nuclear antigen-dependent abasic site repair in *Xenopus laevis* oocytes: an alternative pathway of base excision DNA repair. Mol. Cell. Biol. **14:** 6187–6197.

McAlear, M. A., E. A. Howell, K. K. Espenshade and C. Holm, 1994 PCNA mutations suppress the cell cycle defect conferred by *cdc44* mutations. Mol. Cell. Biol. **14:** 4390–4397.

Mével-Ninio, M., R. Terracol, C. Salles, A. Vincent and F. Payre, 1995 *ovo*, a *Drosophila* gene required for ovarian development, is specifically expressed in the germline and shares most of its

coding sequences with *shavenbaby*, a gene involved in embryo patterning. Mech. Dev. **49:** 83–95.

Montecucco, A., R. Rossi, D. S. Levin, R. Gary, M. S. Park *et al.*, 1998 DNA ligase I is recruited to sites of DNA replication by an interaction with proliferating cell nuclear antigen: identification of a common targeting mechanism for the assembly of replication factories. EMBO J. **17:** 3786–3795.

Mossi, R., Z. O. Jónsson, B. L. Allen, S. H. Hardin and U. Hübscher, 1997 Replication factor C interacts with the C-terminal side of proliferating cell nuclear antigen. J. Biol. Chem. **272:** 1769–1776.

Nichols, A. F., and A. Sancar, 1992 Purification of PCNA as a nucleotide excision repair protein. Nucleic Acids Res. **20:** 2441–2446.

Oku, T., S. Ikeda, H. Sasaki, K. Fukuda, H. Morioka *et al.*, 1998 Functional sites of human PCNA which interact with p21 (Cip1/Waf1), DNA polymerase δ and replication factor C. Genes Cells **3:** 357–369.

Perrimon, N., L. Engstrom and A. P. Mahowald, 1984 The effects of zygotic lethal mutations on female germ-line functions in *Drosophila.* Dev. Biol. **105:** 404–414.

Pirrotta, V., 1997 Chromatin-silencing mechanisms in Drosophila maintain patterns of gene expression. Trends Genet. **13:** 314–318.

Rabinowitz, M., 1941 Studies on the cytology and early embryology of the egg of *Drosophila melanogaster*. J. Morphol. **69:** 1–49.

Rawls, J. M., and J. W. Fristrom, 1975 A complex genetic locus controls the first three steps of pyrimidine biosynthesis in *Drosophila*. Nature **255:** 738–740.

Roiha, H., G. M. Rubin and K. O'Hare, 1988 P element insertions and rearrangements at the *singed* locus of *Drosophila melanogaster*. Genetics **119:** 75–83.

Roos, G., Y. Jiang, G. Landberg, N. H. Nielsen, P. Zhang *et al.*, 1996 Determination of the epitope of an inhibitory antibody to proliferating cell nuclear antigen. Exp. Cell Res. **226:** 208–213.

Sali, A., and T. L. Blundell, 1993 Comparative protein modelling by satisfaction of spatial restraints. J. Mol. Biol. **234:** 779–815.

Sandler, L., D. L. Lindsley, B. Nicoletti and G. Trippa, 1968 Mutants affecting meiosis in natural populations of *Drosophila melanogaster*. Genetics **60:** 525–558.

Schüpbach, T., 1982 Autosomal mutations that interfere with sex determination in somatic cells of *Drosophila melangaster* have no direct effect on the germline. Dev. Biol. **89:** 117–127.

Schüpbach, T., and E. Wieschaus, 1991 Female sterile mutations on the second chromosome of *Drosophila melanogaster*. II. Mutations blocking oogenesis or altering egg morphology. Genetics **129:** 1119–1136.

Shivji, M. K. K., M. K. Kenny and R. D. Wood, 1992 Proliferating cell nuclear antigen is required for DNA excision repair. Cell **69:** 367–374.

Sullivan, W., P. Fogarty and W. Theurkauf, 1993 Mutations affecting the cytoskeletal organization of syncitial *Drosophila* embryos. Development **4:** 1245–1254.

Torres-Ramos, C. A., B. L. Yoder, P. M. J. Burgers, S. Prakash and L. Prakash, 1996 Requirement of proliferating cell nuclear antigen in *RAD6*-dependent postreplication DNA repair. Proc. Natl. Acad. Sci. USA **93:** 9676–9681.

Tsurimoto, T., 1998 A multifunctional ring on DNA. Biochim. Biophys. Acta **1443:** 23–39.

Umar, A., A. B. Buermeyer, J. A. Simon, D. C. Thomas, A. B. Clark *et al.*, 1996 Requirement for PCNA in DNA mismatch repair at a step preceding DNA resynthesis. Cell **87:** 65–73.

Warbrick, E., D. P. Lane, D. M. Glover and L. S. Cox, 1995 A small peptide inhibitor of DNA replication defines the site of interaction between the cyclin-dependent kinase inhibitor $p21^{WAF1}$ and proliferating cell nuclear antigen. Curr. Biol. **5:** 275–282.

Warbrick, E., D. P. Lane, D. M. Glover and L. S. Cox, 1997 Homologous regions of Fen1 and $p21^{Cip1}$ compete for binding to the same site on PCNA: a potential mechanism to co-ordinate DNA replication and repair. Oncogene **14:** 2313–2321.

Weinstein, A., 1936 The theory of multistrand crossing over. Genetics **21:** 155–199.

Wieschaus, E., 1980 A combined genetic and mosaic approach to the study of oogenesis in *Drosophila*, pp. 85–94 in *Development and Neurobiology of Drosophila*, edited by O. Siddiqi, P. Pabu, L. M. Hall and J. C. Hall. Plenum Press, New York.

Yamaguchi, M., Y. Nishida, T. Moriuchi, F. Hirose, C.-C. Hui *et al.*, 1990 Drosophila proliferating cell nuclear antigen (cyclin) gene: structure, expression during development, and specific binding of homeodomain proteins to its 5′-flanking region. Mol. Cell. Biol. **10:** 872–879.

Yamamoto, Y., F. Girard, B. Bello, M. Affolter and W. J. Gehring, 1997 The *cramped* gene of *Drosophila* is a member of the *Polycomb*-group, and interacts with *mus209*, the gene encoding proliferating cell nuclear antigen. Development **124:** 3385–3394.

Yarger, R., and R. C. King, 1971 The phenogenetics of a temperature sensitive, autosomal dominant, female sterile gene in *Drosophila melanogaster*. Dev. Biol. **24:** 166–177.

Zhang, P., Y. Sun, H. Hsu, L. Zhang, Y. Zhang *et al.*, 1998 The interdomain connector loop of human PCNA is involved in a direct interaction with human polymerase δ. J. Biol. Chem. **273:** 713–719.

Communicating editor: V. G. Finnerty